New Worlds Observer Optical Performance

Amy S. Lo, Tiffany Glassman, Chuck Lillie
Northrop Grumman Corporation

ABSTRACT

New Worlds Observer is an external occulter, or, starshade, mission designed to detect visible wavelength (less than 1 micron) light from Earth-like planets around solar neighborhood stars. A telescope spacecraft operates in the "shadow" cast by an starshade spacecraft, located tens of thousands of kilometers away. The specially contoured petals on the starshade spacecraft control the diffraction to produce high contrast suppression of the on-axis starlight. The starshade operates in the Fresnel, or near field, diffraction regime, which adds complexity to numerical simulations of its performance. As a validation of the numerical models and a demonstration of the starshade capabilities, we have built a testbed to measure the performance of subscale NWO hypergaussian starshades. We describe the rationale for our testbed and its set up. We expect to be able to report results from the testbed in a later paper this year.

Keywords: Exo-planet, Occulter, Apodization, Starshade, Testbed, Terrestrial Planet Finder

1. INTRODUCTION

New Worlds Observer (NWO) is a mission concept designed to identify extra-solar planets. NWO consists of a telescope and an external starshade aligned with a target star. A sketch of the NWO architecture is shown in Figure 1.

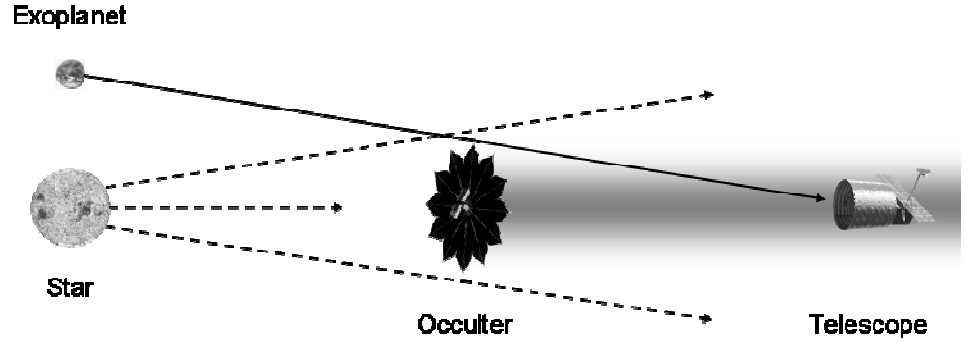

Figure 1: The basic architecture of the NWO mission. A generic telescope is used in conjunction with the NWO starshade to block out the on-axis starlight and detect and characterize an off-axis source – the extra-solar planet.

Detecting and characterizing an Earth-like, extra-solar planet is very difficult. At visible wavelengths, shortward of 1 micron planets are seen by reflected starlight; the small size and relatively low albedo of the planet means that a brightness difference of $\sim 10^{10}$ exists between the star and planet. In addition, the planet and the star are quite close together; at 10 parsecs away, Earth would be only 100 mas from the Sun. These realities create the performance requirements of the system – we need to be able to achieve a very high contrast ratio, very close to the star. The starshade is capable of creating a given contrast ratio for a planet at all angles greater than some minimum, called the Inner Working Angle (IWA).

2. THE BINARY, APODIZED STARSHADE

In a recent paper, Cash (2006) showed that an external starshade with a hypergaussian transmission profile (Equation 1) provides a deep, broadband null for on-axis light and high transmission for an off-axis source. The hypergaussian apodization function $A(\rho)$ is given by:

UV/Optical/IR Space Telescopes: Innovative Technologies and Concepts III
edited by Howard A. MacEwen, James B. Breckinridge
Proc. of SPIE Vol. 6687, 668716, (2007) · 0277-786X/07/$18 · doi: 10.1117/12.730521

$$A(\rho) = 0 \qquad \rho < a$$
$$A(\rho) = 1 - \exp\left[-\left(\frac{\rho - a}{b} \right)^n \right] 0 \qquad \rho \geq a \tag{1}$$

where a is the radius of a central region of zero transmission, b is the fall-off radius of the exponential function, n is the index that determines how quickly the hypergaussian function falls with radius, and ρ is the starshade radius. For more details about how this function was derived and how it creates a dark shadow, see Lo, Glassman, & Arenberg (2007).

The smooth transmission profile can be broken up into P petals, where the average fraction of solid area versus radius is equal to A(ρ). This allows us to build a binary starshade that totally opaque rather than one with variable transmission; a variable transmission occulter is difficult to manufacture. The 1-dimensional apodization function and the 2-dimensional, binary starshade are shown in Figure 2.

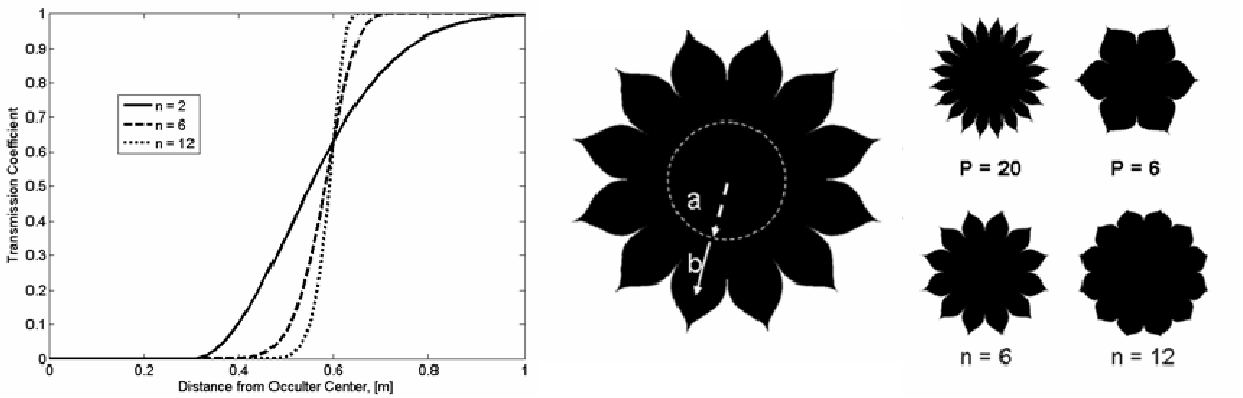

Figure 2: *Left*: The apodization function, A(□), for the NWO starshade, showing several different hypergaussian functions. *Center*: A 12-petaled, binary starshade with n = 6. *Right*: Illustrations of starshade shapes with different petal numbers and values of n.

3. MODELING OF THE STARSHADE PERFORMANCE

Now that we have derived an apodization function, we would like model the detailed performance of the starshade. This will give us a confirmation of the theoretical performance level and a visual representation of the resulting distribution of light.

There are two methods to do this – a numerical simulation of the diffraction of light around the starshade and a lab test involving a sub-scale starshade. These methods are complimentary, as the combination of both will show that the results are robust. The optical simulation and its results are described in detail in Lo et al. (2007). Here we will summarize the key results before focusing on the lab scale model.

3.1. Numerical Simulation

There are two planes of interest in this simulation: the shadow plane and the image plane (see Figure 3). The shadow is a region of high starlight suppression that is big enough to accommodate the aperture of the telescope. We will focus on this plane, since that is where we will be working in the lab test.

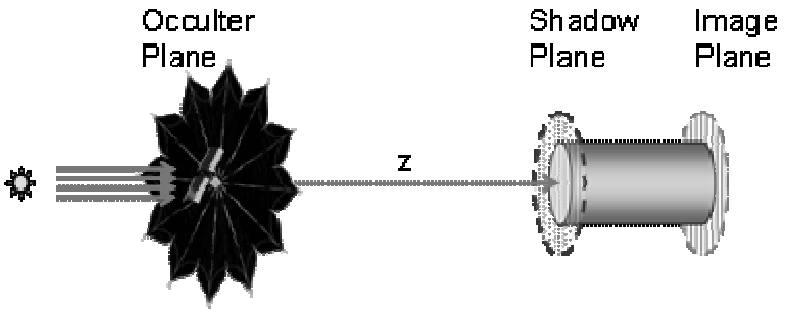

Figure 3: There are two planes of interest in the optical simulation. The incoming radiation strikes the starshade in the "starshade plane" and is diffracted by the starshade. The light forms a deep shadow in the "shadow plane", a distance z away, where the telescope aperture is placed. The telescope then forms an image of the light it collects, which is focused in the "image plane".

The appearance of the shadow, as modeled by the numerical simulation, is seen in Figure 4. The shadow has a very dark, central region that is large enough to accommodate the telescope. Near the edges, diffraction from the petals creates a complex pattern as the intensity rises. Our simulation can model the total depth of the shadow as well as its size and how the light encroaches at the edges.

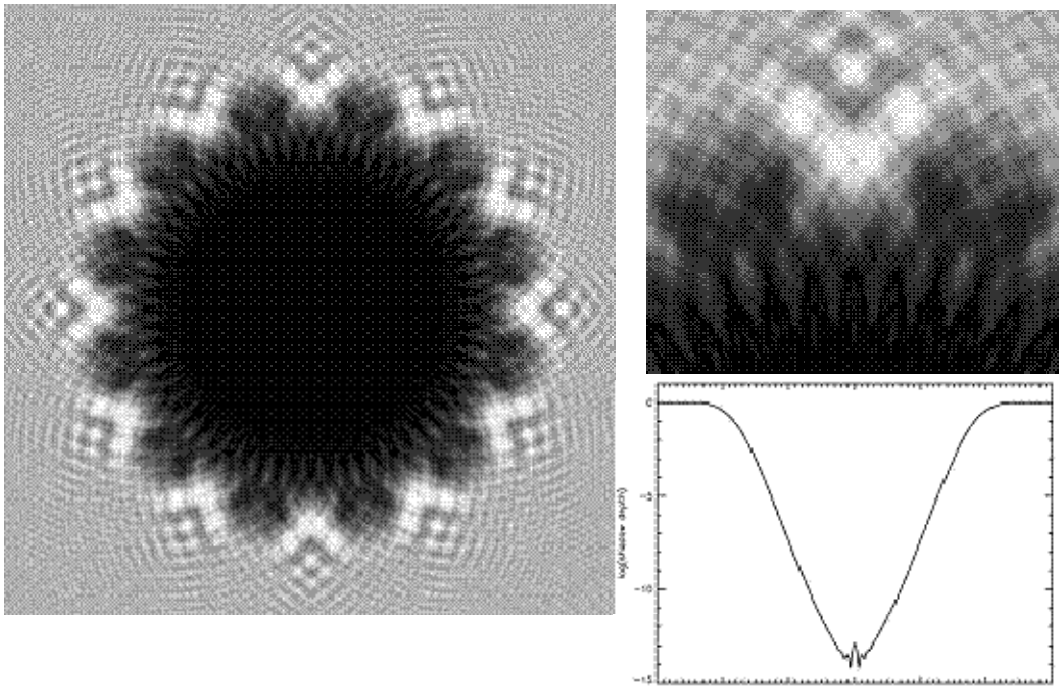

Figure 4: The shadow cast by the starshade is shown on the left. On the right is a blow up of the edge of that shadow and a slice through the shadow showing that the highest contrast regions have a depth of ~1X10^{-13}.

3.1.1. Problems with Numerical Simulations

There are several simplifying assumptions that must go into any numerical simulation in order for the calculation to be tractable. The first assumption we made is that the starshade operates in the Fresnel regime and therefore we can use the Fresnel integral. The full equation describing the diffraction of light is the Rayleigh-Sommerfeld equation:

$$E(x_0, y_0) = \iint_A E(x_1, y_1) \frac{1}{i\lambda r} \exp(ikr) \cos(\bar{n}, \bar{r}) dx_1 dy_1 \qquad (2)$$

where λ is the wavelength of light, k=2π/λ, $\overline{n}$ is the normal vector connecting the aperture plane to the observation plane, and $\overline{r}$ is the radial vector connecting the points (x_1, y_1) and (x_0, y_0).

To be able to solve this equation we make a number of assumptions that are valid in the Fresnel limit. First, we assume that

$$\cos(\overline{n},\overline{r}) \cong 1 \tag{3}$$

which is valid to 5% for angles less than 18 degrees. This restriction is not expected to be violated; given the large distance between the starshade and the telescope, we are only concerned with a small region around the optical axis. Next we take the first term of the binomial expansion of r so that:

$$r = \sqrt{z^2 + (x_0 - x_1)^2 + (y_0 - y_1)^2} \tag{4}$$

becomes:

$$r = z\left[1 + \frac{1}{2}\left(\frac{x_0 - x_1}{z}\right)^2 + \frac{1}{2}\left(\frac{y_0 - y_1}{z}\right)^2\right]. \tag{5}$$

This simplifies equation (2) so that it becomes:

$$E(x_0, y_0) = \frac{e^{ikz}}{i\lambda z}\exp\left[\frac{i\pi}{\lambda z}\left({x_0}^2 + {y_0}^2\right)\right]\iint_A E(x_1, y_1)\exp\left[\frac{i\pi}{\lambda z}\left({x_1}^2 + {y_1}^2\right)\right]\exp\left[\frac{-2i\pi}{\lambda z}\left(x_1 x_0 + y_1 y_0\right)\right]dx_1 dy_1, \tag{6}$$

which is the Fresnel integral. The separation of variables makes this equation is much easier to solve.

The Fresnel integral is valid when solved over the whole aperture, which in this case is the entire sky outside the starshade. We can use Babinet's principle to solve for an equivalent pinhole with the same shape which makes the integral much simpler. Babinet's principle states that the distributions of light resulting from an occulting spot and from the same shaped pinhole in an infinite plane are related by:

$$E_{occulter} = e^{ikz} - E_{pinhole.} \tag{7}$$

Solving the Fresnel equation for a pinhole is much more tractable since the integral is only over the area of the opening. However, using Babinet's principle generally assumes Fraunhoffer conditions. We have performed checks of fields calculated using Babinet's principle and fields calculated using a very large grid, and for simple apertures, they are identical. With a complicated aperture like ours, the correspondence may degrade. Cross checks using numerical simulation are prohibitively CPU intensive.

Our complicated aperture does not have an analytic solution; we must choose a method of solving the Fresnel integral numerically. Solving the integral in a direct, brute force way by numerical integration is too slow to be practical, so further assumptions must be made. One method of solving the integral is to write the Fresnel equation in polar coordinates:

$$E(\rho,\phi) = 1 - \frac{1}{i\lambda z}\int_0^{\infty}\int_0^{2\pi} e^{\frac{i\pi}{\lambda z}\left(r^2 + \rho^2 - 2r\rho\cos(\theta - \phi)\right)} E(r,\theta)\, r\, d\theta\, dr \tag{8}$$

and then expand this equation by the Jacobi-Anger transform:

$$\begin{aligned} E(\rho,\phi) &= 1 - \frac{2\pi}{i\lambda z}\int_0^{R} e^{\frac{i\pi}{\lambda z}\left(r^2 + \rho^2\right)} J_0\left(\frac{2\pi r\rho}{\lambda z}\right)E(r)\, r\, dr \\ &- \sum_{m=1}^{\infty}\frac{2\pi(-1)^m}{i\lambda z}\left(\int_0^{R} e^{\frac{i\pi}{\lambda z}\left(r^2 + \rho^2\right)} J_{mN}\left(\frac{2\pi r\rho}{\lambda z}\right)\frac{\sin\left(\pi m E(r)\right)}{\pi m}\, r\, dr\right) X\left(2\cos\left(mN\left(\phi - \frac{\pi}{2}\right)\right)\right) \end{aligned} \tag{9}$$

where J_{mN} are Bessel functions of order mN, and N is the number of petals in the starshade. In order to use this expansion, a finite number of terms must be taken. If enough terms are chosen, this approaches the full equation.

Another way to solve the Fresnel integral numerically is to use a Fast Fourier Transform (FFT) technique. This technique uses the similarity between the last term of Equation (6) and the FFT:

$$E_{p,q} = \sum_{m=0}^{M-1} \sum_{n=0}^{N-1} E_{m,n} \exp\left[-2i\pi\left(\frac{mp}{M} + \frac{nq}{N}\right)\right]. \quad (10)$$

The Fresnel integral can therefore be solved by taking the FFT of the input light distribution, along with a phase factor. While very fast, the primary limit of this technique is that a large grid must be used to represent the starshade to the required accuracies. Given finite computer resources and time, the size of the grid that can be used to calculate the sum is limited. In addition, the FFT itself involves certain simplifications and errors that are well documented elsewhere (see e.g. Cooley & Tukey 1965).

The assumptions that must be made to do optical simulations have been checked and any errors they impose are believed to be well below the level of accuracy needed. However, any numerical model should be tested against reality to make sure that the fundamental physics behind the models is valid.

3.2. Sub-scale starshade lab test

The best way to test if the assumptions we made in the numerical simulation are valid is to do a laboratory test of the system. This will tell us the actual behavior of an starshade responding to real photons. The size of the full flight system for NWO (an starshade that is 30 to 50 meters in diameter operated 30,000 to 80,000 km from the telescope) prevents us from doing a full-scale test. Instead, we can test a system with the same Fresnel number as the full scale system. The Fresnel number is defined as:

$$F = \frac{R^2}{\lambda z}, \quad (11)$$

where R is the radius of the starshade and z is the distance from the starshade to the detector. This value specifies the behavior of the system – a setup with the same Fresnel number will have the same diffraction behavior. If the full scale starshade has R = 25 m, z = 80,000 km, and operates at wavelengths shorter than 800 nm, the Fresnel number of the system will be 10 to 15. Since we want to do the subscale test in visible light as well, the size and distance of the starshade will have to be scaled together to keep the Fresnel number about the same.

We are limited by the size of the facility we can use and the size of test starshade that be constructed to represent the figure accuracy of the actual starshade. The smallest test starshade we can accurately build is ~20 mm in radius (see section 3.2.2). Therefore, to match the Fresnel number, the test distance must be 45 to 65 m.

3.2.1. Previous Lab Experiment

Webster Cash and collaborators at the University of Colorado were the first to perform a version of this experiment. They created a test starshade that is 45 mm in diameter and tested it in a dark tunnel that was 45 m long. It was illuminated by sunlight that was piped into the system by a heliostat. They measured a suppression of the starlight of 10^{-7} (Cash 2006). This is still 3 orders of magnitude less than expected from this setup.

We believe that the two primary reasons for the Cash shadow depth limit are:

1) The experiment was in conducted in air, so dust and air currents could scatter the light from the bright outer regions of the shadow into the dark inner regions, washing out the shadow depth.
2) The test starshade manufacturing process left errors in the shape of the starshade that cause scattered light and a lower contrast shadow.

3.2.2. Current Testbed Setup

The Northrop Grumman microelectronics facility is capable of high precision wafer manufacturing and we can therefore attempt to improve on the Cash results by using higher fidelity test starshades. By adapting the wafer construction processes, we can develop a test starshade that has approximately 1/1000 to 1/10,000 figure accuracy, which is the level

we believe is needed for the NWO starshade. Once a good test starshade is available, we recreated the basics of the Cash set up with the exception that we designed for vacuum capabilities.

The test starshade patterns are etched on a Si substrate, with a photoresist layer that is then metalized. Various metallization options were explored, and an alternating layer of NiCr and Au was the best solution for a stable final product with minimum warping. The substrate is then thinned and etched to reveal the final starshade. The resulting test starshade is approximately 40 mm in diameter, with edges features smaller than 0.5 micron, and high metrological accuracy. The truncation point of the starshade is variable from tip to tip, with some of them tapering down to less than 1 micron.

Unique to the NWO starshade design is the fact that its suppression is panchromatic. The starshade is designed for adequate performance at the longest wavelength necessary, and is capable of similar levels of suppression on all shorter wavelengths. Its bandpass is therefore very large, well over 100%. For example, our test starshade is designed to give a contrast suppression of 10^{-10} at 800 nm; it is expected to perform as well or better at shorter wavelengths, and in white light. This will be an important part of our test.

3.2.3. Construction and Calibration of the Testbed

We have constructed a 60 m long vacuum tube out of 0.3 m diameter PVC pipes. These are bolted together in 3 meter segments and mounted on sawhorses (see Figure 6). The tubes are lined with aluminum inserts that are painted black to minimize scattered light in the tubes. There are also baffles placed at many locations along the tube that are designed to further cut down on scattered light. The ends of the tube have aluminum caps with 5 cm diameter quartz windows to let the beam through.

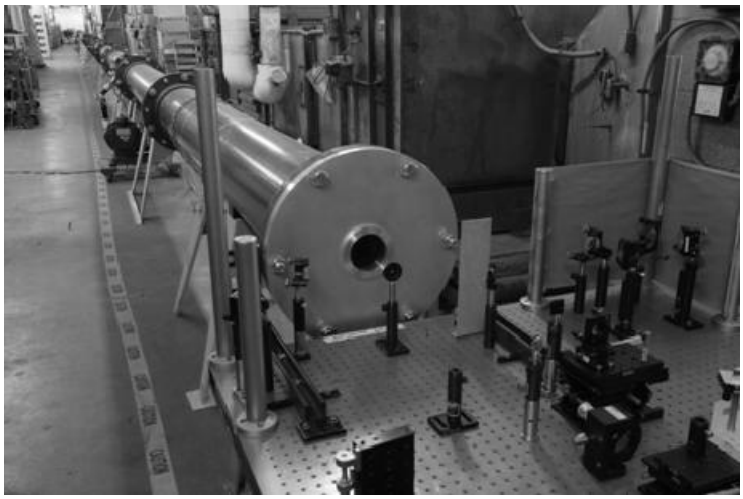

Figure 6: The testbed vacuum tube showing the source-end optical bench and the vacuum pump in the background. The entire tube is 60 m in length.

The starshade is mounted in a sealable box halfway down the tube (Figure 7). The starshade itself is glued to a mounting screw that is held into a ring using three guitar wires. The starshade assembly can be used to rotate the starshade from outside of the tube to test the effects tilting the starshade.

Figure 7: On the right is the test starshade mounted in a ring by guitar strings. On the left a cloth has been placed in the system so that the light distribution and the shadow of the starshade can be seen.

The light source we are using is currently a Nd:YAG laser with an additional fainter HeNe laser to help with alignment. As with all long baseline optical experiments, keeping the beam aligned is our biggest optical challenge: a small adjustment of the set up causes the beam to become misaligned. Thermal distortions and building vibrations requires us to realign the system before each measurement. We therefore have placed several sets of mirrors to 1) determine the magnitude and source of misalignment, and 2) adjust the beam in position and pointing with high precision (Figure 8). There is a pinhole just before the entrance to the tube that is used to clean up the wavefront of the beam. We have a weak halogen source for white light alignment, but need a brighter lamp for proper illumination of the starshade.

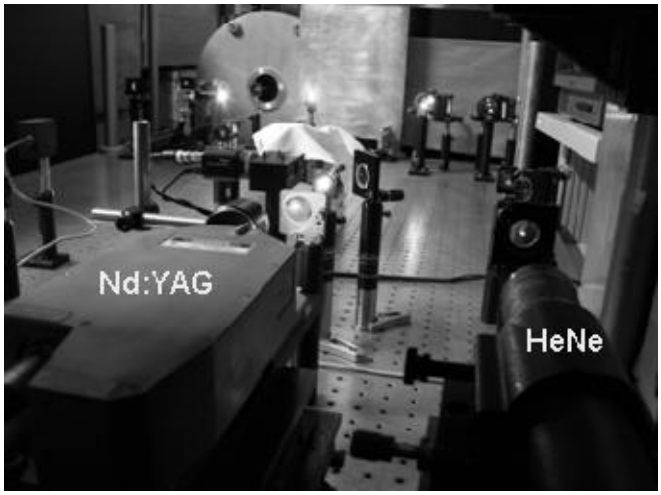

Figure 8: The source-end optical table is seen with the entrance to the vacuum tube in the background. The two lasers that are being used as a light source (the Nd:YAG) and an alignment laser (the HeNe) are seen in the foreground.

The detector we are using is an SBIG CCD camera with a very small field of view so there is no contamination from the bright areas of the starshade shadow. It does not contain a lens, and is used to capture the photon distribution of the shadow plane. It is water cooled to -30°C. The optical bench at the detector end also contains several other cameras and monitors that are used in aligning the system (Figure 9).

Figure 9: The setup on the detector end is shown. The science detector is mounted up against the end of the vacuum tube on the right. There is a small telescope, another small camera, two monitors for use in aligning the system. The laptop on the left will be used to take the data.

There is a vacuum pump just past the source end of the tube (Figure 6) that can reach 1/10 atm in less than 30 minutes and 1/50 atm in less than 1 hour. The persistence rate is better than 1/1000 atm per hour.

3.2.4. Preliminary Testbed Results

Figure 10 shows an image taken with the testbed that is a mosaic of 36 exposures. This image has a very good correspondence to the results of the numerical simulation (see Figure 4). The main difference is a series of diffraction rings that are present in the testbed data, which we believe are the result of a continued misalignment in the system that is causing the beam to clip a baffle. This is one of the issues we are continuing to work on.

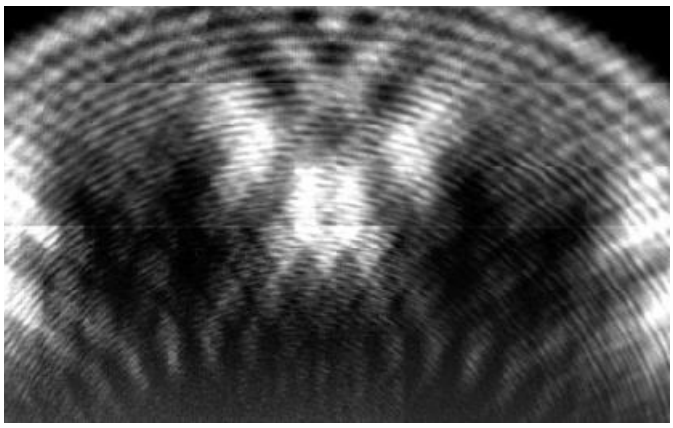

Figure 10: An image of the edge of the shadow of the starshade taken in the testbed. This image is a mosaic of 36 images, each of which is a 1 millisecond exposure.

3.2.5. Estimated Obtainable Results

For our testbed setup, with 600 nm light, the best case would give us an average contrast in the camera of ~$1X10^{-9}$. The deepest portions of the shadow should have a suppression of ~$1X10^{-14}$ in this case. There are several factors that would degrade this performance. In order of their estimated impact, these include:

- Non-uniform wavefront from the light source. We expect that we should be able to achieve a wavefront that is uniform to at least 1 part in 10^3 and hopefully as good as 1 part in 10^5. From the numerical simulation, we expect that for wavefront errors of 10^{-5}, the deepest portions of the shadow would have a contrast no better than ~$1X10^{-10}$. For errors of 10^{-4} the highest contrast would be ~$1X10^{-8}$ and for errors of 10^{-3} it would be ~$1X10^{-6}$.
- Stray light getting into the beam path. We hope to mitigate this to a large extent so that it is no longer an issue.
- Manufacturing errors on the starshade shape. Though the starshade manufacturing process is very good, there will be some remaining non-uniformities. From our numerical simulation, we expect that if the edge errors are no bigger than 1 part in 10,000, the suppression would only be impacted at the level of $1X10^{-10}$. We think the starshade errors are close to this level already, so there shouldn't be a significant impact from this issue. In addition, by carefully measuring the errors that do exist on the starshade edge, we can verify the predictions of the numerical simulation for how the errors will affect the performance.

3.2.6. Future Work

The next step in this process is to mitigate the effects above to get some results out of the current testbed setup. In the future, we would also like to improve the testbed by getting:

- A more sensitive detector, so that we can measure the shadow at very low light levels with adequate S/N.
- A better light source that is bright enough to give sufficient S/N in the shadow and provide a uniform beam. It should also be a white light source instead of a laser to better match the spectrum from a real star and to mitigate issues we are currently having with the coherence of the laser.
- A more stable environment to reduce vibration and thermal effects.

4. CONCLUSION

NWO is a unique mission concept using a binary, apodized, external starshade. Although numerical simulations can be used to model the performance of this starshade, building a testbed to check the simulation is an important step. If the two methods give results that are in agreement, the performance of the starshade will be fully convincing.

We have built a testbed for the starshade that consists of a 60 m-long vacuum chamber and a 40 mm diameter test article. We have a laser light source and a CCD camera as a detector. We are currently in the process of understanding and improving the behavior of the testbed. We expect to get a measurement very soon of the suppression level achieved by this starshade. In addition to debugging the current testbed, there are several improvements that can be made to the testbed in the future to improve its performance.

5. REFERENCES

Cash, W. 2006, Private Communication

Cooley, J. W. & Tukey, J.W. 1965, Mathematics of Computation, 19, 297

Lo, A. S., Glassman, T. G. & Arenberg, J. 2007, ApJ, submitted